Journal of Alloys and Compounds 509 (2011) 2294–2299

Contents lists available at ScienceDirect

Journal of Alloys and Compounds

journal homepage: www.elsevier.com/locate/jallcom

CTAB-assisted hydrothermal synthesis of tungsten oxide microflowers

Oranuch Yayapao[a], Titipun Thongtem[a,*], Anukorn Phuruangrat[b,*], Somchai Thongtem[c]

[a] Department of Chemistry and Center for Innovation in Chemistry, Faculty of Science, Chiang Mai University, Chiang Mai 50200, Thailand
[b] Department of Materials Science and Technology, Faculty of Science, Prince of Songkla University, Hat Yai, Songkhla 90112, Thailand
[c] Department of Physics and Materials Science, Faculty of Science, Chiang Mai University, Chiang Mai 50200, Thailand

ARTICLE INFO

Article history:
Received 6 September 2010
Received in revised form 25 October 2010
Accepted 28 October 2010
Available online 10 November 2010

Keywords:
Hydrothermal reaction
o-WO_3 microflowers
Optical properties

ABSTRACT

Orthorhombic tungsten oxide (o-WO_3) was synthesized by 200 °C, 24 h hydrothermal reactions of ammonium metatungstate hydrate solutions containing different volumes of 1 M HCl and cetyltrimethylammonium bromide (CTAB) cationic surfactant. The as-synthesized products were characterized by X-ray powder diffraction (XRD), Fourier transform infrared (FTIR) and Raman spectroscopy, and scanning and transmission electron microscopy (SEM, TEM), including UV–visible and photoluminescent (PL) spectroscopy. These analyses showed that their phases and morphologies were controlled by the acidity of the solutions. In 7.50 ml 1 M HCl-added solution, the product was o-WO_3 microflowers, with microsquare layers growing out of their cores. FTIR and Raman vibrations of W=O, O–W–O, and W–O–W stretching modes were detected, and showed typical crystalline WO_3. Their optical properties showed a maximum absorption at 275 nm in the UV region and a maximum emission peak at 375 nm. The possible formation mechanism of o-WO_3 microflowers was also proposed according the experimental results.

1. Introduction

Presently, many chemists and materials scientists are paying close attention to the study of nanostructured oxides – including zero-dimensional (0D) quantum dots, one-dimensional (1D) nanowires and nanorods, and two-dimensional (2D) nanosheets and nanodisks – because these materials have novel physical and chemical properties which are different from their corresponding bulks [1–3]. Among the different oxides with nanostructures, tungsten oxide (WO_3) has received wide attention owing to its unique photochromic and electrochromic properties. It is considered to be a promising material for multiple potential applications, including semiconductors for gas sensors, electrodes for secondary batteries, solar energy converters, and photocatalysts [3–6]. A number of synthetic methods have been developed for WO_3 such as a hydrothermal/solvothermal route [2,3,5,7], thermal processing [4], electric heating in vacuum [6], and physical/chemical vapor deposition process [8,9]. Among these, synthesis under hydrothermal conditions is a low-temperature, environmentally benign and low-cost route for preparation of nanosized oxide materials, and is becoming an increasingly attractive method [10].

In the present research, orthorhombic tungsten oxide (o-WO_3) microflowers were synthesized using a CTAB-assisted hydrothermal method. The as-synthesized o-WO_3 products were further characterized by X-ray powder diffraction (XRD), Fourier transform infrared (FTIR) and Raman spectroscopy, and scanning and transmission electron microscopy (SEM, TEM), including UV–visible (UV–vis) and photoluminescent (PL) spectroscopy.

2. Experiment

A 1.38 g of ammonium metatungstate hydrate ($(NH_4)_6H_2W_{12}O_{40}\cdot xH_2O$) was dissolved in 20 ml deionized water; 0–7.50 ml 1 M HCl was subsequently added to form H_2WO_4 with 30 min continuous stirring. CTAB surfactant (0.36 g) was added to each solution with an additional 30 min of continuous stirring. The mixtures were transferred into homemade, Teflon-lined, stainless steel autoclaves. These were tightly closed, heated at 200 °C for 24 h, and naturally cooled to room temperature. Finally, light-green precipitates were synthesized, separated by filtration, washed with deionized water and ethanol, and dried at 70 °C for 12 h.

The products were characterized and recorded on a Philips X'Pert MPD X-ray diffractometer (XRD) equipped with a graphitic monochromator of Cu Kα radiation (λ = 0.1542 nm), using a scanning rate of 0.02°/s over the 2θ range of 10–60°. FTIR spectra were recorded on PerkinElmer Spectrum RX FTIR Spectrometer with KBr as a diluting agent and operated in the range of 400–4,000 cm^{-1} with the resolution of 4 cm^{-1}. Raman vibrations of the products were detected by a HORIBA JOBIN YVON T64000 Raman spectrometer with 50 mW and 514.5 nm wavelength Ar laser. Field-emission scanning electron microscopic (FE-SEM) images were taken by a JEOL JSM-6335F operated at 15.0 kV beam energy. Transmission electron microscopic (TEM) images, and selected area electron diffraction (SAED) pattern were taken on a JEOL JEM-2010, employing at an accelerating voltage of 200 kV. UV–visible and photoluminescent spectra were carried out by a Lambda 25 spectrometer using UV lamp with the resolution of 1 nm, and LS50B Fluorescence Spectrometer, PerkinElmer, at 450 W Xe-lamp with the 0.2 nm resolution and 200 nm excitation wavelength at room temperature.

* Corresponding authors. Tel.: +66 0 53 943344; fax: +66 053 892277.
E-mail addresses: ttpthongtem@yahoo.com (T. Thongtem), phuruangrat@hotmail.com (A. Phuruangrat).

0925-8388/$ – see front matter © 2010 Elsevier B.V. All rights reserved.
doi:10.1016/j.jallcom.2010.10.204

3. Results and discussion

Fig. 1 shows the XRD patterns of the products synthesized by 200 °C, 24 h hydrothermal reactions using $(NH_4)_6H_2W_{12}O_{40}{\cdot}xH_2O$ and CTAB as a tungsten source and surfactant, with 0–7.50 ml 1 M HCl added. In the HCl-free solution, the product was an amorphous phase. When 2.50 ml 1 M HCl was added to the solution, both orthorhombic $WO_3{\cdot}0.33H_2O$ (JCPDS No. 35-0270) and WO_3 phases (JCPDS No. 20-1324) [11] were detected. These products became pure orthorhombic WO_3 (o-WO_3) in the 5.00 ml and 7.50 ml 1 M HCl-added precursor solutions. The analysis implies that HCl has an influence on the synthesis of pure o-WO_3 phase.

SEM images (Fig. 2a and b) show o-WO_3 in the shape of ~8 μm microseeds in numerous square layers in the 5.00 ml 1 M HCl-added solution. By increasing 1 M HCl from 5.00 ml to 7.50 ml, these microsquare layers grew out of the microseed cores to form microflower-like particles (Fig. 2c and d), composed of 2–3 μm × 100–300 nm × 100–300 nm petals with very smooth surfaces.

In general, o-WO_3 has a distorted ReO_3-type structure consisting of a three-dimensional network of WO_6 octahedrons linked by their oxygen corners [5,12]. The vibrations are in the infrared (IR) range, and are classified into three regions: 600–900, 200–400 and <200 cm^{-1}, corresponding to O–W–O stretching and bending modes, and lattice vibration, respectively [13]. In this research, the products (Fig. 3) were further characterized by FTIR spectroscopy in the range of 400–4000 cm^{-1}, and the vibrations compared to those of CTAB. Some bands were detected at 2800–3020 cm^{-1}, which can be attributed to the CTAB surfactant. The FTIR spectrum of CTAB shows two intense bands at 2918 and 2846 cm^{-1}, corresponding to the asymmetric and symmetric stretching vibrations of C–CH_2 in the methylene chains. The sharp bands at 1450–1500 cm^{-1} were specified as the deformation of –CH_2– and –CH_3, and the weak band at 3011 cm^{-1} as the C–CH_3 asymmetric stretching and N–CH_3 symmetric stretching vibrations of the solid surfactant [14–17]. In case of the as-synthesized products, broad bands between 590

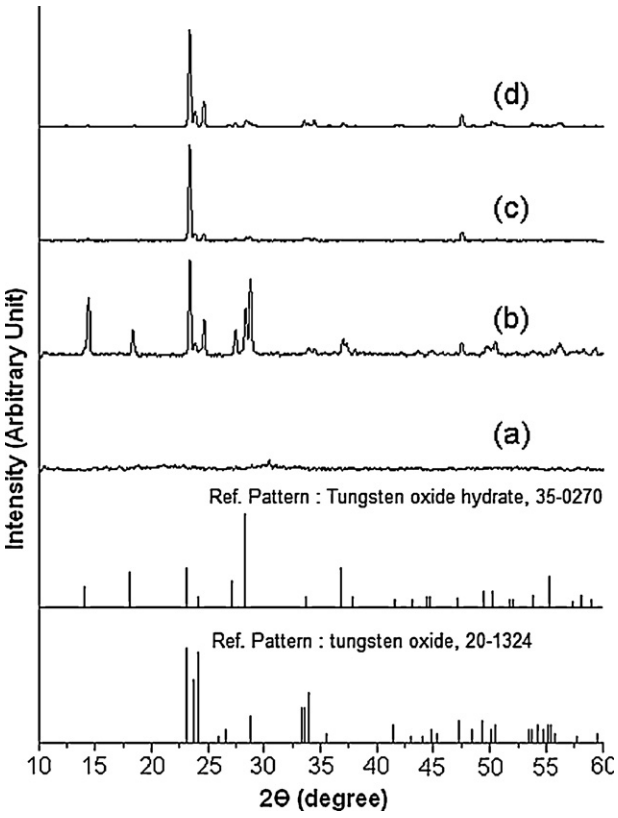

Fig. 1. XRD patterns of the products synthesized by the hydrothermal reaction at 200 °C for 24 h in the respective solutions containing (a–d) 0.00 ml, 2.50 ml, 5.00 ml, and 7.50 ml of 1 M HCl, as compared to the JCPDS standard patterns of orthorhombic WO_3 $0.33H_2O$ and WO_3 [11].

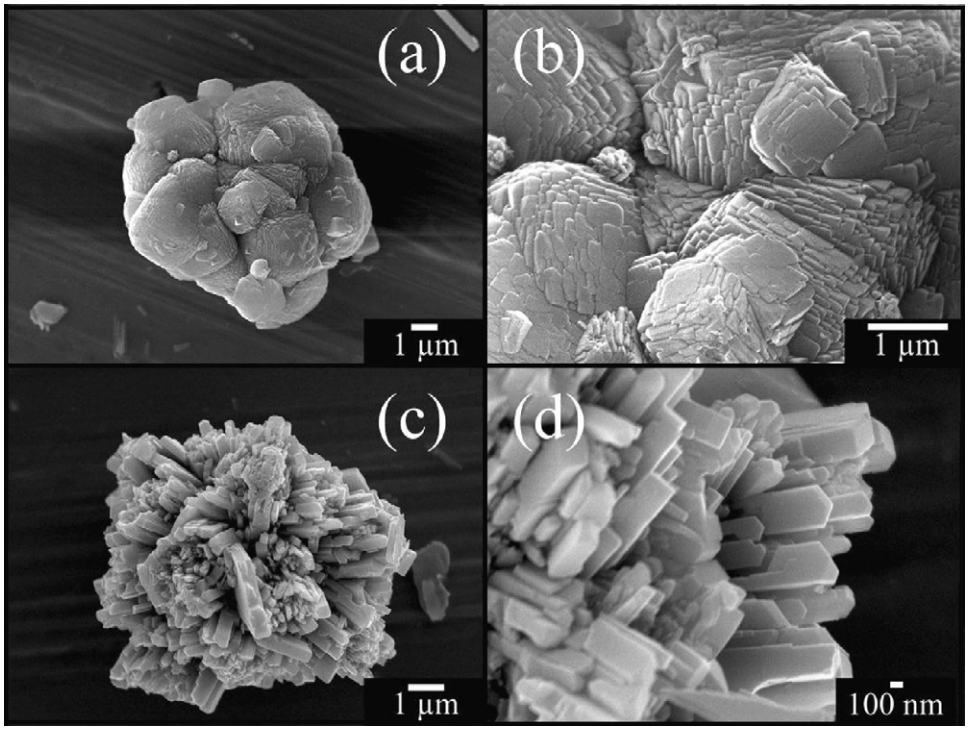

Fig. 2. SEM images of o-WO_3 synthesized by the hydrothermal reaction at 200 °C for 24 h in the solutions containing (a, b) 5.00 ml, and (c, d) 7.50 ml of 1 M HCl.

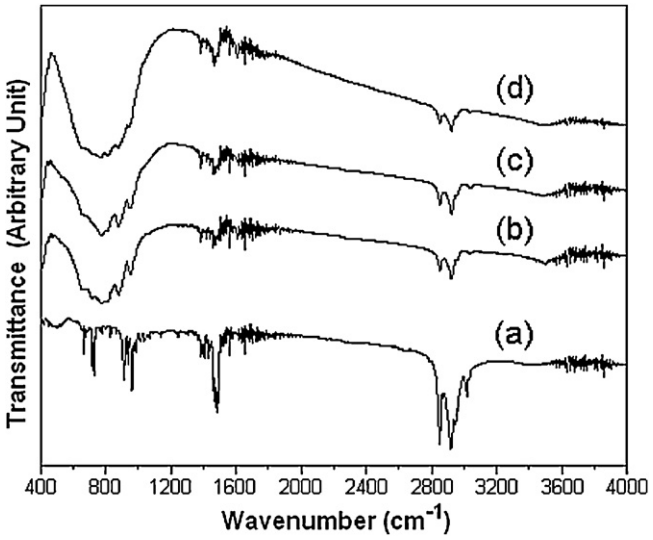

Fig. 3. FTIR spectra of (a) CTAB, and (b–d) the products synthesized by the hydrothermal reaction at 200 °C for 24 h in the solutions containing 2.50 ml, 5.00 ml, and 7.50 ml of 1 M HCl, respectively.

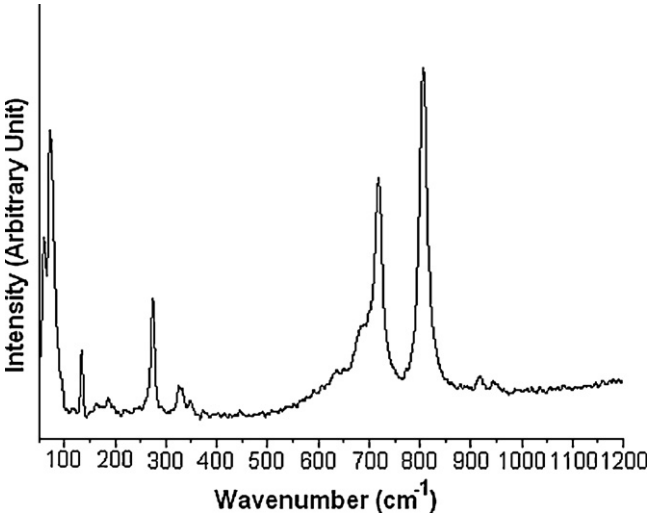

Fig. 4. Raman spectrum of o-WO_3 microflowers, synthesized by the hydrothermal reaction at 200 °C for 24 h in the solution containing 7.50 ml 1 M HCl.

and 949 cm^{-1} were detected. They are attributed to the stretching of short W=O bonds, while the bands at 817 and 728 cm^{-1} were assigned to be the O–W–O stretching modes. The vibrational bands centered at 659 and 590 cm^{-1} were attributed to the W–O–W stretching modes [5]. The asymmetric and symmetric stretching vibrations of CH_2 in the methylene chains of the incorporated CTAB were also detected at the same wavenumbers as those of the solid surfactant – implying that no intermolecular interaction was enhanced due to the capping effect, and the conformation of methylene chains remained unchanged. Their intensities are weakened, because CTAB was not completely removed by washing with deionized water and ethanol, and remained as the adsorbed head groups on the surfaces of these products – as was also found in previous reports [14,15,17].

The Raman spectrum of the as-synthesized WO_3 microflowers over the range of 50–1200 cm^{-1} is shown in Fig. 4. Generally, the 950–1050 cm^{-1} Raman wavenumbers of the transition metal oxide are assigned to be the symmetric stretching modes of metal and oxygen bonds (short terminal W=O, ν_s(W=O) terminal bands), and 750–950 cm^{-1} bands were either the antisymmetric stretching of W–O–W bonds (ν_{as}(W–O–W)) or symmetric stretching of –O–W–O– bonds (ν_s(–O–W–O–)). The Raman spectrum of the as-synthesized WO_3 microflowers detected vibrational peaks at 806, 718, 686, 326, 274, 134, 76 and 60 cm^{-1}. The two main intense peaks at 806 and 718 cm^{-1}, and the shoulder at 686 cm^{-1}, are typical Raman peaks of crystalline WO_3, which correspond to the stretching and bending vibrations of the bridging tungsten and oxygen atoms. They are assigned to be the W–O stretching (ν), W–O bending (δ) and O–W–O deformation (γ) modes, respectively. Two peaks at 326 and 274 cm^{-1} are assigned to be the bending δ(O–W–O) vibrations. Those below 200 cm^{-1} modes were attributed to the lattice vibrations. All these peaks are in good accordance with those of other reports [1,5,12,18,19].

Detailed morphology of the as-synthesized o-WO_3 structure was proved by TEM images (Fig. 5), which show the product shape to be microflowers 6–8 μm in diameter; these are composed of a large number of petals with lengths up to several micrometers. Some petals were released from the microflower cores by ultrasonic vibrations during preparation of the samples for TEM analysis. Fig. 6a and b presents high-magnification TEM images with the *x*-axis of Fig. 5b tilted. These o-WO_3 petals are straight and smooth, with uniform dimension along their axial direction. The selected area electron diffraction patterns (Fig. 6c and d) were indexed and specified as orthorhombic WO_3 phase (JCPDS No. 20-1324) [11],

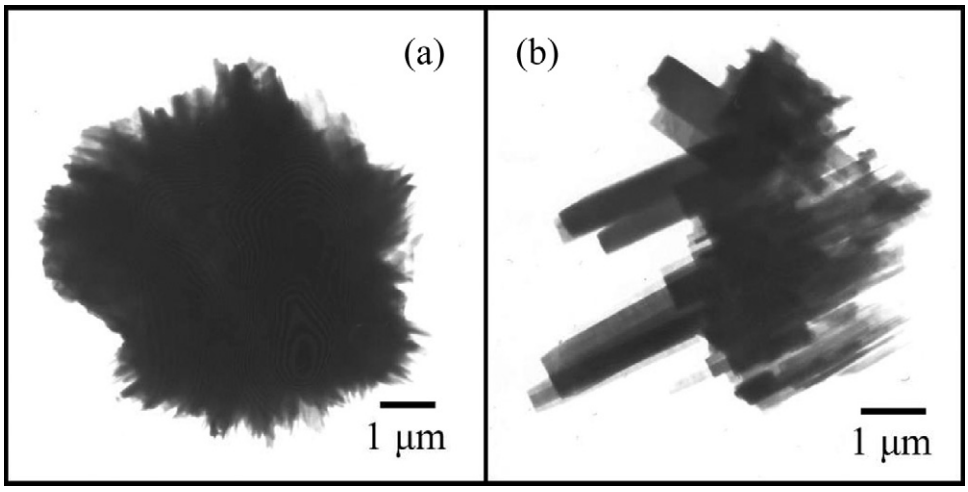

Fig. 5. TEM images of o-WO_3 microflowers, synthesized by the hydrothermal reaction at 200 °C for 24 h in the solution containing 7.50 ml 1 M HCl.

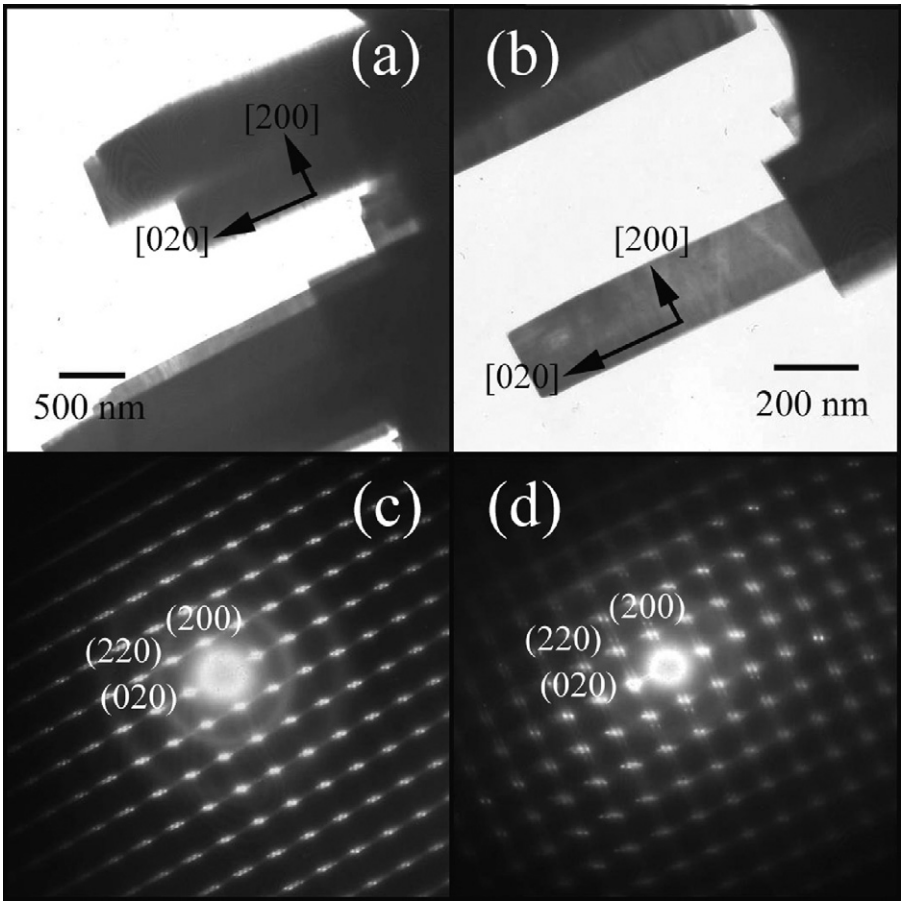

Fig. 6. (a, b) High magnification TEM images, and (c, d) SAED patterns of o-WO_3 microflowers of Fig. 5(b).

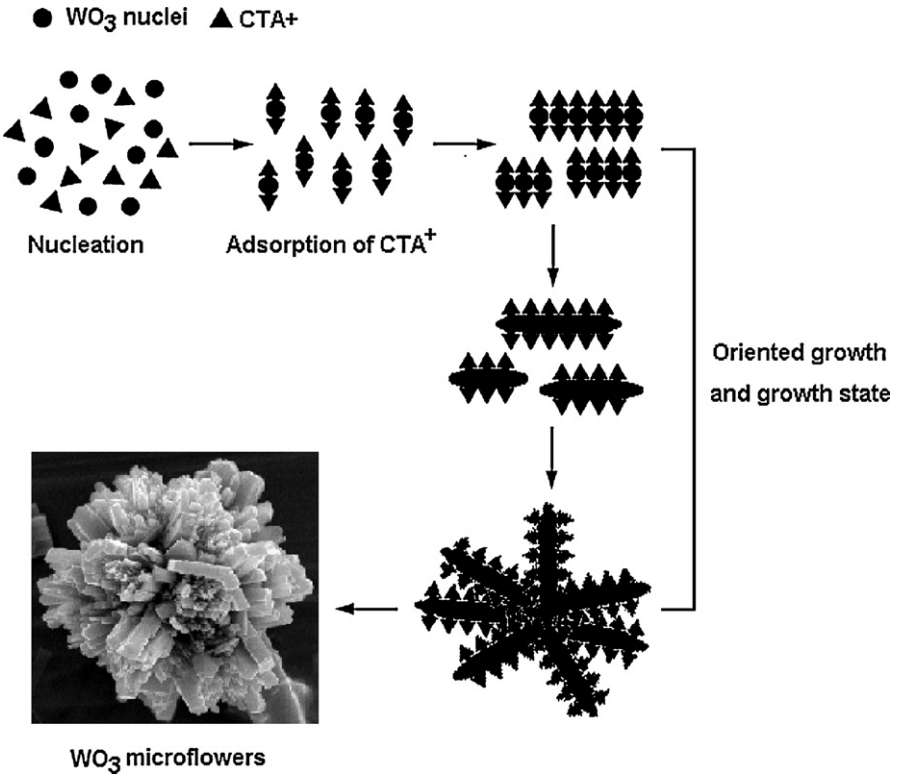

Fig. 7. Schematic diagram for the formation of o-WO_3 microflowers.

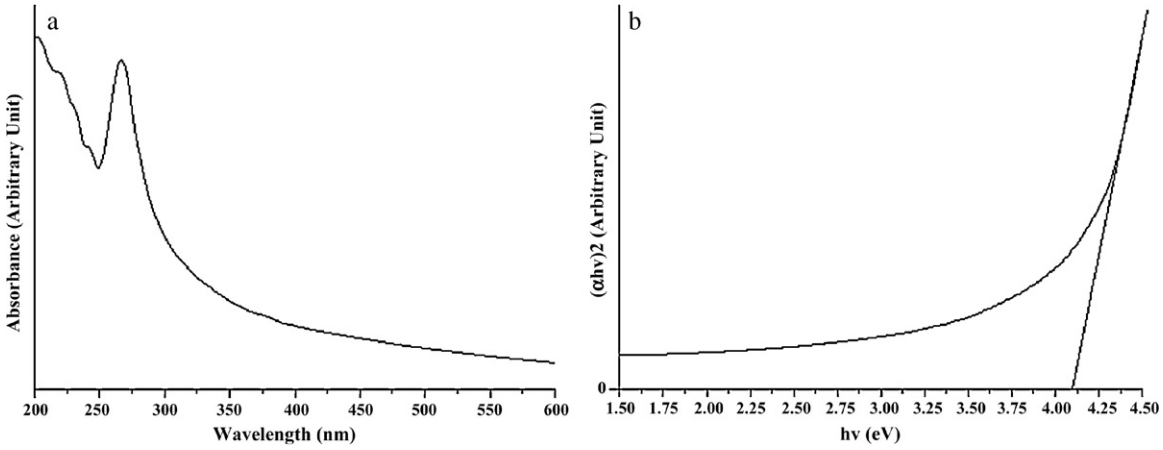

Fig. 8. (a) UV–visible spectrum, and (b) the $(\alpha h\nu)^2$ versus $h\nu$ plot of o-WO_3 microflowers, synthesized by the hydrothermal reaction at 200 °C for 24 h in the solution containing 7.50 ml 1 M HCl.

in accordance with the XRD analysis. They show the (0 2 0), (2 2 0) and (2 0 0) diffraction planes with the electron beam in the [0 0 −1] direction. It should be noted that the growth direction of the petals is normal to the (0 2 0) plane of the microsquare layers – implying that the o-WO_3 microsquare layers are aligned along the [0 2 0] direction.

The formation of o-WO_3 microflowers can be explained by polycondensation, electroneutral and dehydration reactions from the polyoxotungstate anions, as shown below:

$$H_2W_{12}O_{40}{}^{6-} + 6H^+ + (8+n)H_2O \rightarrow 12H_2WO_4 \cdot nH_2O \quad (1)$$

$$H_2WO_4 \cdot nH_2O \rightarrow \text{o-}WO_3(\text{nuclei}) + (n+1)H_2O \quad (2)$$

$$\text{o-}WO_3(\text{nuclei}) \rightarrow WO_3(\text{microflowers}) \quad (3)$$

When $(NH_4)_6H_2W_{12}O_{40}{\cdot}xH_2O$ was dissolved in deionized water, followed by the addition of HCl, the colorless solution of $H_2W_{12}O_{40}{}^{6-}$ anions changed to $H_2WO_4{\cdot}nH_2O$ yellow precursor precipitates. Upon the 200 °C hydrothermal reaction, $H_2WO_4{\cdot}nH_2O$ was further decomposed to produce o-WO_3 (nuclei) [20–22], containing in microsquare layers of $[WO_6]^{6-}$ octahedrons [5,12] lying in the [2 0 0] direction. At this stage, CTAB – which is a positively charged cationic surfactant (CTA^+) with a long hydrophobic tail [14,23,24] – was attracted by the four negatively charged oxygen atoms in the planar surface of $[WO_6]^{6-}$, due to the stereochemical effect. The $[CTA\text{–}WO_6]^{2-}$ bonds orientated parallel to the [0 2 0] direction inhibited growth in the [2 0 0] and [0 0 2] directions because of the CTA^+ hydrophobic tails [21,23]. The $[CTA\text{–}WO_6]^{2-}$ petals grew out from cores to form o-WO_3 microflowers, and the CTAB molecules were washed out, as shown in Fig. 7.

UV–vis absorbance for o-WO_3 microflowers (Fig. 8a) shows an absorption band in the 200–450 nm range and a strong band at 275 nm, attributed to the high UV spectrum [25]; this might be a consequence of the confined nature of electrons in the [0 1 0] direction [1]. No absorption band in the visible range was detected. This result is in accordance with those reported by Nataraj and co-workers [18], and Xu and co-workers [25]. The direct band gap (E_g) of o-WO_3 microflowers was determined by Eq. (4):

$$\alpha h\nu = (h\nu - E_g)^n \quad (4)$$

where α, h, ν, and E_g are the absorbance, Planck constant, photon frequency, and optical band gap, respectively. The parameter n is a pure number associated with the different types of electronic transitions: $n = 1/2, 2, 3/2$ or 3 for direct–allowed, indirect–allowed, direct–forbidden and indirect–forbidden transitions, respectively [26]. Its direct energy gap was determined by extrapolation of the linear portion of the curve (Fig. 8b) to $\alpha = 0$, corresponding to 4.10 eV. It should be noted that the change of absorption was controlled by two photon energy ($h\nu$) ranges – the high and low energies. When the photon energy is greater than the energy band gap (E_g), absorption was linearly increased with the increasing of photon energy. But for the photon energy with less than E_g, the absorption became different from the linearity, due to the dominant photonic absorption relating to defect levels between the valence and conduction bands of the product.

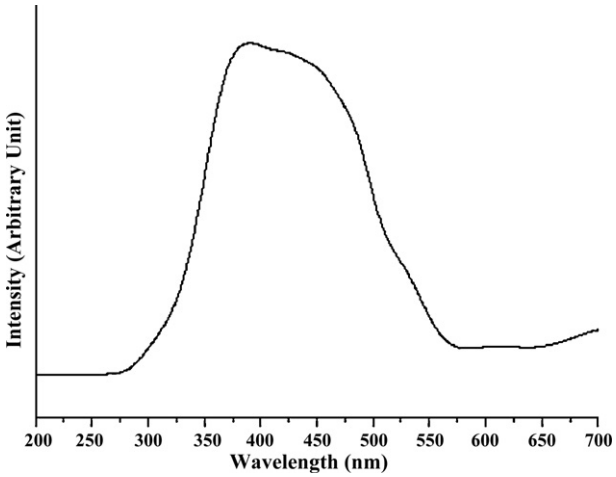

Fig. 9. PL spectrum of o-WO_3 microflowers.

The PL spectrum (Fig. 9) of the as-synthesized o-WO_3 microflowers was recorded using 200 nm excitation wavelength at room temperature. The emission peak presents a broad band at 275–575 nm with a maximum emission at 375 nm in the violet region by Gaussian curve fitting, due to the electronic transition of WO_3. This PL emission is in accordance with the report of Lee and co-workers [27].

4. Conclusions

In summary, o-WO_3 microflowers composing of long petals (E_g = 4.10 eV) were successfully synthesized by the CTAB-assisted hydrothermal reaction at 200 °C for 24 h. Their microsquare layers grew along the [0 2 0] direction to form the petals. UV spectrum shows a maximum absorption at 275 nm, and PL emission at 375 nm.

Acknowledgements

This research was supported by the National Nanotechnology Center (NANOTEC), a member of National Science and Technology Development Agency (NSTDA); Ministry of Science and Technology; Thailand Research Fund (TRF); and Center for Innovation in Chemistry (PERCH-CIC), Commission on Higher Education (CHE), Ministry of Education, Thailand.

References

[1] A. Wolcott, T.R. Kuykendall, W. Chen, S. Chen, J.Z. Zhang, J. Phys. Chem. B 110 (2006) 25288–25296.
[2] A. Yan, C. Xie, D. Zeng, S. Cai, M. Hu, Mater. Res. Bull. 45 (2010) 1541–1547.
[3] Z. Gu, Y. Ma, W. Yang, G. Zhang, J. Yao, Chem. Commun. (2005) 3597–3599.
[4] S. Sun, Y. Zhao, Y. Xia, Z. Zou, G. Min, Y. Zhu, Nanotechnology 19 (2008) 305709.
[5] S. Salmaoui, F. Sediri, N. Gharbi, Polyhedron 29 (2010) 1771–1775.
[6] D.Z. Guo, K. Yu-Zhang, A. Gloter, G.M. Zhang, Z.Q. Xue, J. Mater. Res. 19 (2004) 3665–3670.
[7] Y. Bi, D. Li, H. Nie, Mater. Chem. Phys. 123 (2010) 225–230.
[8] Y.B. Li, Y. Bando, D. Golberg, K. Kurashima, Chem. Phys. Lett. 367 (2003) 214–218.
[9] P. Tägtström, U. Jansson, Thin Solid Films 352 (1999) 107–113.
[10] Y. Li, X. Su, J. Jian, J. Wang, Ceram. Int. 36 (2010) 1917–1920.
[11] Powder Diffract File, JCPDS-ICDD, 12 Campus Boulevard, Newtown Square, PA, U.S.A.
[12] I.M. Szilágyi, J. Madarász, G. Pokol, P. Király, G. Tárkányi, S. Saukko, J. Mizsei, A.L. Tóth, A. Szabó, K. Varga-Josepovits, Chem. Mater. 20 (2008) 4116–4125.
[13] C. Guéry, C. Choquet, F. Dujeancourt, J.M. Tarascon, J.C. Lassègues, J. Solid State Electrochem. 1 (1997) 199–207.
[14] Z.M. Sui, X. Chen, L.Y. Wang, L.M. Xu, W.C. Zhuang, Y.C. Chai, C.J. Yang, Physica E 33 (2006) 308–314.
[15] H. Kavas, Z. Durmus, M. Şenel, S. Kazan, A. Baykal, M.S. Toprak, Polyhedron 29 (2010) 1375–1380.
[16] G. Wang, Q. Mu, T. Chen, Y. Wang, J. Alloys Compd. 493 (2010) 202–207.
[17] Y.D. Wang, S. Zhang, C.L. Ma, H.D. Li, J. Lumin. 126 (2007) 661–664.
[18] S. Rajagopal, D. Nataraj, D. Mangalaraj, Y. Djaoued, J. Robichaud, O.Y. Khyzhun, Nanoscale Res. Lett. 4 (2009) 1335–1342.
[19] J. Díaz-Reyes, R.J. Delgado-Macuil, V. Dorantes-García, A. Pérez-Benítez, J.A. Balderas-López, J.A. Ariza-Ortega, Mater. Sci. Eng. B 174 (2010) 182–186.
[20] E.V. Timofeeva, G.A. Tsirlina, O.A. Petrii, Russ. J. Electrochem. 39 (2003) 716–726.
[21] A. Phuruangrat, D.J. Ham, S. Thongtem, J.S. Lee, Electrochem. Commun. 11 (2009) 1740–1743.
[22] Z. Jiao, X.W. Sun, J. Wang, L. Ke, H.V. Demir, J. Phys. D: Appl. Phys. 43 (2010) 285501.
[23] X.M. Sun, X. Chen, Z.X. Deng, Y.D. Li, Mater. Chem. Phys. 78 (2002) 99–104.
[24] T. Thongtem, S. Kaowphong, S. Thongtem, Appl. Surf. Sci. 254 (2008) 7765–7769.
[25] Q. Xiang, G.F. Meng, H.B. Zhao, Y. Zhang, H. Li, W.J. Ma, J.Q. Xu, J. Phys. Chem. C 114 (2010) 2049–2055.
[26] J.C. Sczancoski, L.S. Cavalcante, N.L. Marana, R.O. da Silva, R.L. Tranquilin, M.R. Joya, P.S. Pizani, J.A. Varela, J.R. Sambrano, M.S. Li, E. Longo, J. Andrés, Curr. Appl. Phys. 10 (2010) 614–624.
[27] J. Wang, P.S. Lee, J. Ma, J. Cryst. Growth 311 (2009) 316–319.